CEBAF Program Advisory Committee Six (PAC6) Proposal Cover Sheet

This proposal must be received by close of business on April 5, 1993 at:

CEBAF
User Liaison Office
12000 Jefferson Avenue
Newport News, VA 23606

Proposal Title

The Charged Pion Form Factor

Contact Person

Name: David J. Mack
Institution: CEBAF
Address: MS 12H
Address: 12000 Jefferson Ave.
City, State ZIP/Country: Newport News, VA 23606 U.S.A.
Phone: (804) 249-7442 **FAX:** (804) 249-7363
E-Mail → BITnet: MACK@CEBAF **Internet:**

If this proposal is based on a previously submitted proposal or letter-of-intent, give the number, title and date:

CEBAF Use Only

Receipt Date: 4/5/93 Log Number Assigned: PR 93-021

By: _____

CEBAF Proposal:

The Charged Pion Form Factor

D.Abbott*, R.Carlini, D.Mack (Spokesperson), D.Meekins*, J.Mitchell,
S.Wood, W.Vulcan, C.Yan
Physics Division, CEBAF

O.K.Baker, S.Beedoe, L.G.Tang
Physics Department, Hampton University,
and Physics Division, CEBAF

A.Klein
Old Dominion University

G.Adams, J.Napolitano, P.Stoler
Physics Department, Renssalaer Polytechnic Institute

H.Mkrtchyan, A.Gasparyan, Ts.Amatuni, R.Badalian
Yerevan Physics Institute

* *Also affiliated with the Physics Department,*
College of William and Mary.

Abstract

We propose a separation of all unpolarized structure functions for forward pion electroproduction on the nucleon at Q^2 = .5 - 5. $(GeV/c)^2$. Assuming the dominance of t-channel one pion exchange in the charged pion forward longitudinal response, the pion charge form factor F_π can be determined. The measurements of F_π proposed here would dramatically improve on the existing data set and provide an important test of soft predictions in the transition between soft and perturbative regimes. Model tests are proposed as well to search for physics backgrounds which may be present in the longitudinal response near $-t_{min}$ for our kinematics. The proposed measurements will also readily distinguish between two extreme versions of the $g_{\pi NN}$ form factor, a matter of recent controversy.

1 Introduction

One of the great hopes for research at CEBAF is that it lead to a better understanding of QCD between the non-perturbative and perturbative regimes. Improvement in our knowledge of F_π, the pion charge form factor, would be an important step. Although the pion is not an easy experimental target, it is a simpler object than the nucleon. Perturbative QCD descriptions of elastic form factors should be valid at much lower Q^2 for the pion than for the nucleon since the former contains one fewer quark. In fact, for $Q^2 \simeq 5$ $(GeV/c)^2$, roughly half of the F_π amplitude may be due to PQCD contributions. Another feature which makes the pion case particularly interesting is that the pion β-decay constant f_π normalizes the asymptotic form factor Q^2F_π. No such independent normalization exists for G_M^P, which is a function of the (unknown) proton structure function. Existing data on G_M^P at up to Q^2=30 $(GeV/c)^2$ are also believed by some authors to be very far from asymptotia.

New data for F_π covering the Q^2 range .5 - 5. $(GeV/c)^2$ with combined statistical, systematic, and model errors of order 10% would dramatically improve the F_π data base, and would allow one to distinguish between existing treatments of soft contributions. We expect our errors to be even smaller at the lower Q^2 values where kinematics considerations allow us to approach the pion pole rather closely.

1.1 Formalism

To make F_π measurements at low Q^2, pion beams have been scattered from atomic electrons. Employing 50-300 GeV pions, results have been obtained at Q^2 = .013 - .28 $(GeV/c)^2$. [1] These data determine the slope of the form factor near Q^2=0, and therefore the charge radius. The values of the pion rms radius from the later Fermilab and CERN SPS experiments (.66 fm) are in good agreement.

The only way to measure F_π at high Q^2 is to use virtual pions emitted from light nuclear targets. Large energy transfers are necessary since they allow one to closely approach the pion pole and suppress rescattering through baryon resonances.

Figure 1 defines the coordinate system which we use to discuss pion electroproduction. The scattering plane is defined by $\vec{P}_e \times \vec{P}_{e'}$, with $\vec{q}$ the three-momentum transfer. Several important center of momentum variables are then defined with respect to the scattering plane and $\vec{q}$: θ_π is the polar angle between $\vec{p_\pi}$ and $\vec{q}$, and ϕ_π is the angle between $\vec{p_\pi}$ and the scattering plane.

We may write the helicity independent cross section as [2]:

$$\frac{d^5\sigma}{d\Omega_e dP_{e'} dt d\phi} = \Gamma(\frac{d\sigma_T}{dt} + \epsilon\frac{d\sigma_L}{dt} + \epsilon\frac{d\sigma_P}{dt}cos2\phi_\pi + \sqrt{2\epsilon(1+\epsilon)}\frac{d\sigma_I}{dt}cos\phi_\pi)$$

where

$d\sigma^T/dt \equiv \sigma_T$ is the transverse response,
$d\sigma^L/dt \equiv \sigma_L$ is the longitudinal response,
$d\sigma^P/dt \equiv \sigma_P$ is the polarization response,
$d\sigma^I/dt \equiv \sigma_I$ is the longitudinal-transverse interference response,

$$\Gamma = \frac{\alpha}{2\pi^2}\frac{(W^2-M^2)}{2MQ^2}\frac{E'}{E}\frac{1}{1-\epsilon}$$

and

$$1/\epsilon = 1 + \frac{2|\vec{q}|^2}{Q^2}\tan^2\theta_e/2.$$

where M is the nucleon mass, W is the invariant mass in the $\gamma_v + p$ system, $Q^2 \equiv -q^2 = -(P_e - P_{e'})^2$ is the 4-momentum transfer, and $E(E')$ is the initial (final) electron energy.

The Feynman or Born diagrams for pion electroproduction are shown in Figure 2. From left to right the diagrams have s-channel, t-channel, and u-channel poles. The Mandelstam variable t, the 4-momentum transfer, has a simple interpretation for the center figure as the mass squared of the virtual pion. In terms of measured quantities, $-t$ can be written as

$$-t = Q^2 - m_\pi^2 + 2\omega E_\pi - 2|\vec{q}||\vec{p_\pi}|cos\theta_\pi.$$

The quantity $-t$ is always positive in electroproduction, and the minimum value is reached when $\theta_\pi \simeq 0$. For kinematics in which the pion pole diagram dominates σ_L (ie, $Q^2 \gg -t \simeq m_\pi^2$) we have [3]

$$\sigma_L \simeq K(eg)^2\frac{-2tQ^2}{(t-m_\pi^2)^2}F_\pi(Q)^2$$

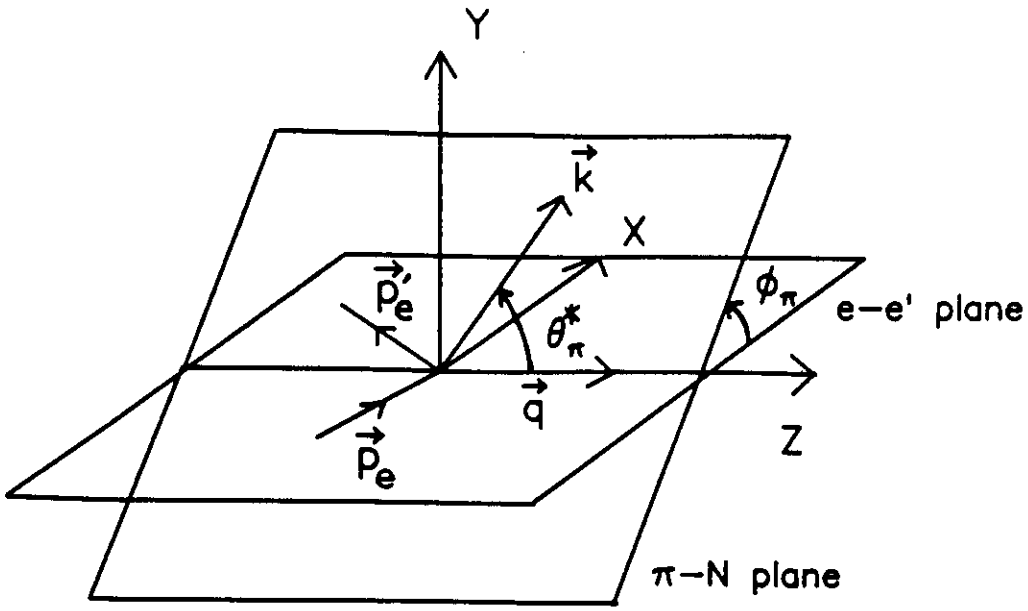

Figure 1: Definition of kinematic variables in electroproduction.

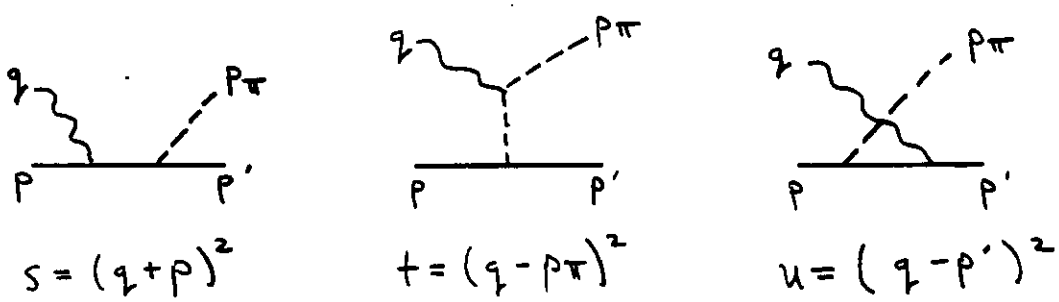

Figure 2: Feynman diagrams for charged pion electroproduction.

where K is a kinematic factor, and e and g are the electromagnetic and strong coupling constants, respectively.

Although the location of the pole at $-t = -m_\pi^2$ is not kinematically accessible in electroproduction, one can approach the pole quite closely, and for $-t \simeq +m_\pi^2$ the value of F_π can be determined from σ_L using the above equation with essentially no model dependence. This will be the case for our lowest Q^2 points. At the higher Q^2 points which we propose, $-t_{min}$ will increase due to CEBAF beam energy limitations. Any physics backgrounds present in σ_L will become relatively more significant as one moves away from the pole. We propose two tests for such backgrounds, so we will be able to estimate the reliability of our F_π extraction. In practice, we will always use a full Born approximation model to extract a value for F_π from the data. For the count rate estimates in this proposal, however, we will use only the pion pole contribution to σ_L.

The pion pole diagram proceeds via isovector photons. In general, however, pion electroproduction may proceed by isoscaler or isovector photons. (Neglecting an isotensor amplitude which appears to be ruled out by experiment.) In very simplified notation, the amplitudes may be written [4]

$$< \pi^+ n|A|\gamma_v p >= A_V + A_S$$

and

$$< \pi^- p|A|\gamma_v n >= A_V - A_S.$$

In this experiment we will measure σ_L near $-t_{min}$. In the limit $-t \rightarrow 0$ we would only be sensitive to other t-pole diagrams. The experimental ratio $\sigma(\pi^+)/\sigma(\pi^-)$ should give an indication of the presense of such isoscaler backgrounds, provided nature has not set the relative phase of these amplitudes to $\pi/2$.

1.2 Previous Experiments

1.2.1 Data

Although this field has been dormant since the late 1970's, the field was quite mature at that time. Hence, we briefly review here some of the hard lessons learned by our predecessors.

The first major work largely above the baryon resonance region (W > 2 GeV) was by Brown *et al.* at the Cambridge Electron Accelerator ("CEA"). [5] The longitudinal response could not be extracted model independently since only high ϵ data were taken. The model of Berends [6] which assumes purely isovector photons was fitted to the unseparated $\sigma_T + \epsilon\sigma_L$ data with F_π as the only free parameter. Between this and a similar experiment at Cornell by Bebek *et al.*[7] ("Cornell I"), values of F_π were obtained for Q^2 = .18 - 2.01 $(GeV/c)^2$.

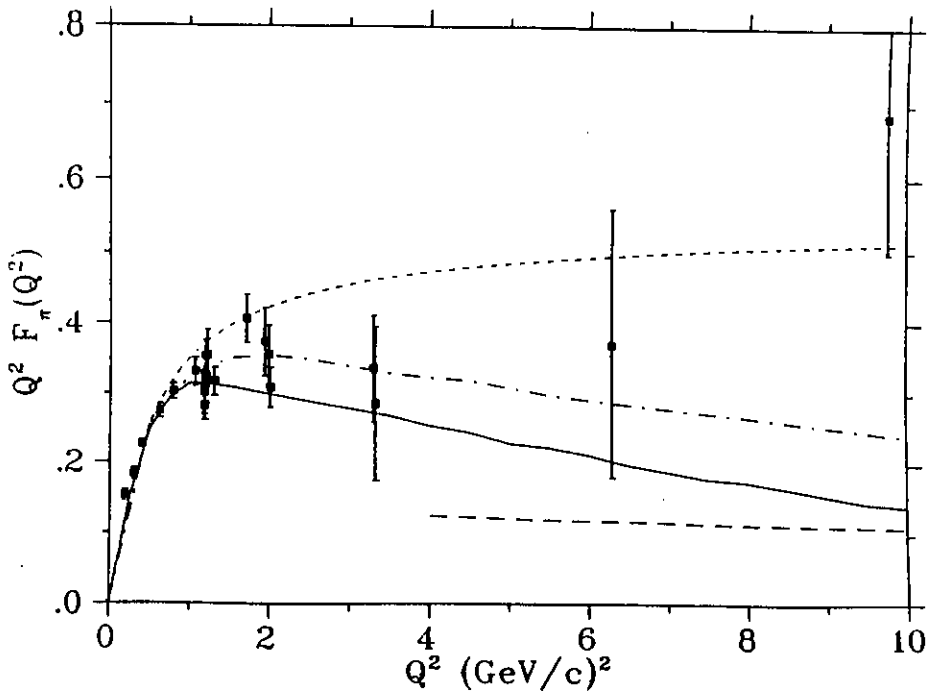

Figure 3: F_π from electroproduction measurements (Cornell III). The short dashed curve is a monopole form factor fitted by Amendolia *et al.* to very low Q^2 elastic pion-electron scattering. See text regarding other curves.

Later work at Cornell ("Cornell II") on a deuterium target demonstrated that a significant isoscalar component existed in the unseparated response, $\sigma_T + \epsilon\sigma_L$ [8]. Because it was believed this isoscalar component should be subtracted before comparison to the model, the old CEA and Cornell I values of F_π were reanalyzed and lowered by 3%-7% with the smaller (larger) corrections at the smaller (larger) end of the Q^2 range. Hence the Cornell II analysis superseded the older CEA and Cornell I analyses.

The next Cornell experiment ("Cornell III") acquired only low ϵ data, but by using earlier high ϵ measurements where available (CEA, Cornell I, and Cornell II) they separated σ_T and σ_L for the first time. It was discovered that the model of Berends grossly underpredicted σ_T at $Q^2 > 1$ $(GeV/c)^2$. Although the poor description of σ_T did not have a large effect on F_π at low Q^2 where $\sigma_L \gg \sigma_T$, the model error meant that the Cornell II F_π values were still too high. The Cornell III values for F_π, valued for their large Q^2 coverage, are found in Figure 3.

No subtraction of isoscaler backgrounds was made in the Cornell III analysis; it was assumed that the isoscaler backgrounds identified in the unseparated Cornell II data were primarily of transverse nature. While Cornell III data provide perhaps the best available estimates at these Q^2 values, large extrapolations in W and Q^2 (between different experiments!) were required. Indeed, it is fair to say that no real measurements of σ_L exist at Q^2 above 3.33 $(GeV/c)^2$.

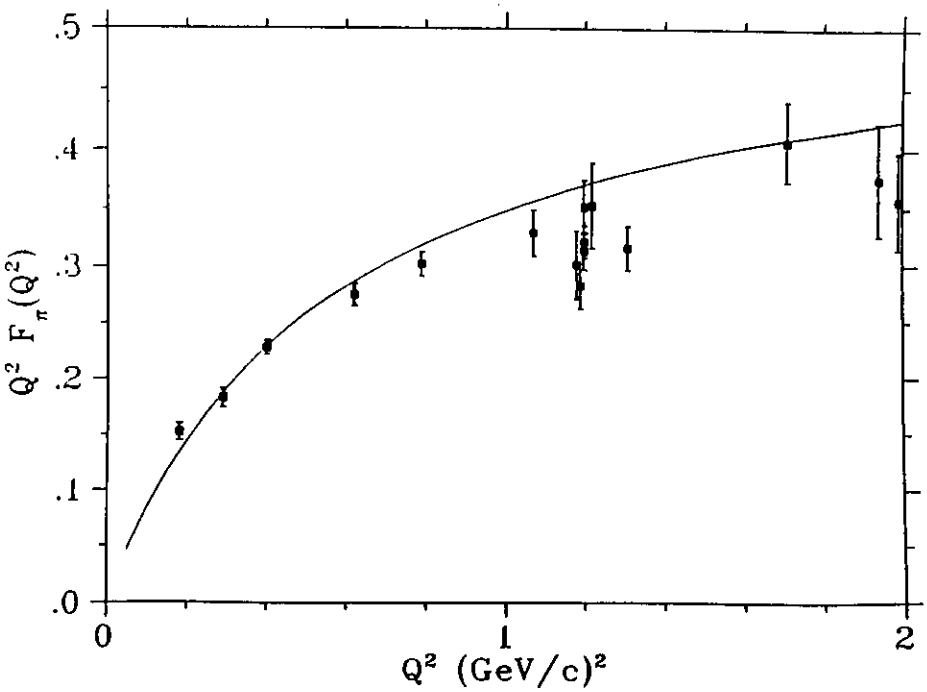

Figure 4: F_π at low Q^2. The solid line is a monopole form factor fitted by Amendolia *et al.* to elastic pion-electron scattering.

1.2.2 Model Tests

It is of some interest to compare F_π derived from electroproduction and elastic scattering measurements. The lowest electroproduction point at $Q^2 = .18$ lies about 2.3 standard deviations above a monopole fit through the elastic data. (Figure 4) Above the Q^2 range of the elastic measurements, however, there are points at Q^2= .29, .4, .62, and .79 all which agree extremely well with the monopole fit. This gives us some confidence that the extraction of F_π from electroproduction data is not pathologically model dependent, at least in this Q^2 region.

One might wonder whether a measurement on a bound nucleon in deuterium gives the same result as on a free nucleon. Bebek *et al.* [8] have shown that, to within their statistical errors, the yield of π^+ at Q^2=1.2 and small $-t$ is the same for both targets. No corrections were made in the analysis other than to use a wider missing mass cut for the deuterium target to account for Fermi motion.

One piece of evidence that backgrounds in σ_L are small, and that t-pole dominance applies at not-so-small values of $-t$, is seen in Figure 5. [8]. Using *unseparated* data, the experimenters determined F_π at two Q^2 values, using data covering a wide range of $-t_{min}$ values. For example, at Q^2=2, consistent values of F_π were obtained using kinematic settings such that $-t_{min}$ ranged from -3.5m_π^2 to -8m_π^2. This latter value is quite far from the pole, and gives us confidence that we may be able to do even better using data with *separated* σ_L.

We turn now to the ratios $\sigma(\pi^-)/\sigma(\pi^+)$. If there are no isoscaler backgrounds, then we

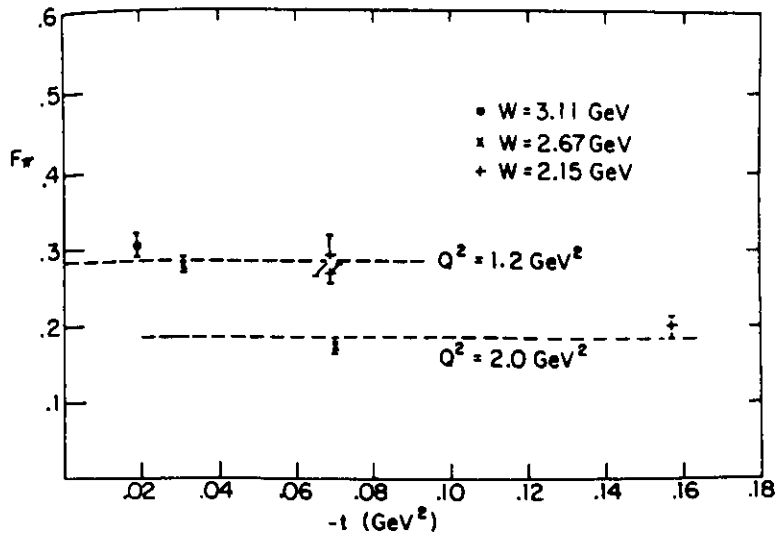

Figure 5: Dependence of the extracted F_π on $-t_{min}$. From Cornell II.

expect R_L= 1. Existing electroproduction data [2] show the *unseparated* ratio R at $-t = .1$ to be slightly less than 1, decreasing at larger values of $-t$. (The errors are of order $\pm 10\%$) While these data are consistent with a two-component model in which $R_L = 1$ at small $-t$ where σ_T dominates, and $R_T \simeq .25$ at large $-t$ where σ_L has died away, they are nevertheless inconclusive. Separated ratios R_L would be much more sensitive to the presense of isoscaler backgrounds.

With increasing Q^2, backgrounds due to interactions with valence quarks must become more important. Nachtman [10] has predicted that s-channel quark diagrams will cause R_T to approach 1/4. This is because π^- production is due to interaction with d quarks (q=1/3) and π^+ with u quarks (q=2/3), so $R_T \propto ((1/3)/(2/3))^2 = 1/4$. The *separated* ratio R_T has been obtained with very large error bars [2], and the data weakly support $R_T = 1/4$. More accurate measurements of R_T (and R_L) would help us to understand the reaction mechanism for pion electroproduction at high Q^2.

1.3 Theory

1.3.1 F_π Predictions

Isgur and Llewellyn Smith [11] have argued that so-called hard (PQCD) contributions to the nucleon magnetic form factor G_M^N are only of order 1% for $Q^2 = 4$ $(GeV/c)^2$. Similar arguments by the same authors suggest that hard contributions to F_π at the same Q^2 may be of order 50%. The reason for this is that while at least two gluons must be exchanged to hold the nucleon together during elastic scattering, a single gluon must be exchanged

in the case of the pion. Each gluon exchange makes the Q^2 needed to achieve the PQCD limit higher by the factor $(\alpha_s/\pi)^{-n}$, where n is the number of exchanged gluons, and α_s is the QCD coupling constant. This suggests that the pion may be the better laboratory for PQCD inspired studies of elastic form factors. Data at higher Q^2 than can be achieved at CEBAF, say Q^2= 15, could test even the most conservative estimates of asymptotic F_π.

Accurate F_π data in the CEBAF Q^2 region of this proposal would provide important tests of QCD in the non-perturbative regime. Estimates of soft contributions by Isgur *et al.* [11] exhibit simple, testable features which lie within reach of CEBAF Q^2 range. The calculations predict a steep rise between 0 and 1.5 $(GeV/c)^2$, where a peak is reached. Above this peak the predictions decrease slowly. (See Figure 3, dot-dash curve.) Radyushkin and collaborators have performed QCD sum rule calculations of the pion wave function and charge form factor F_π. [12, 13] Their calculations relate F_π to parameters of the pion wave function called nonlocal condensates. CEBAF measurements would be directly comparable to such sum rule calculations also.

Jacob and Kisslinger [14] have attempted to describe F_π using a Bethe-Salpeter equation. Their model consists of a linear confining potential which dominates at low Q^2 and a perturbative part which dominates at high Q^2. The asymptotic prediction is that of Farrar and Jackson [15], (long dashed line, Figure 3), and is a rigorous QCD result. The three free parameters of the model (the quark mass, the strength parameter, and the strong coupling constant) are fixed by the normalization $F_\pi(0)$=1.0, the pion decay constant f_π, and the pion rms radius $< r_\pi^2 >^{1/2}$. Thus the model must trivially agree with the F_π data at low Q^2, will describe F_π at asymptotic Q^2 if QCD is valid, and may describe the data at intermediate Q^2 if the model and approximations are any good. The interesting prediction is made (see figure 3, solid line) that Q^2F_π will peak near Q^2=1 and decrease fairly rapidly with Q^2, becoming essentially asymptotic by Q^2=15. Above Q^2=1 the poor quality data suggest, if anything, that the calculation decreases too rapidly. Better quality data are clearly needed for $Q^2 \geq 1$. A Bethe-Salpeter equation model has also been investigated by Ito *et al.* [16]

Lattice gauge calculations have had some modest success in describing F_π at $Q^2 \leq 1$ [18]. Nevertheless, statistical and systematic errors in the calculations are large compared to the data in the range. There are presently no plans to extend these calculations to higher Q^2 [19], although this would be very interesting.

To summarize, much can be learned at CEBAF about the usefulness of QCD sum rule and relativistic potential model applications to the pion in the (presumably) difficult and non-perturbative Q^2 regime of 1 - 5 $(GeV/c)^2$.

1.3.2 Model Dependence

Carlson and Milana [20] have concluded that certain PQCD diagrams may make significant contributions to σ_L as one moves away from the pole. At the $-t_{min}$ of the Cornell experiments, four PQCD diagrams were estimated to contribute 12-18% as much as the Born term at Q^2 of 1.94 to 3.33 $(GeV/c)^2$. It may be possible to determine whether such PQCD backgrounds exist by examining the ratio R_L, discussed above. It is an experimental fact that the unseparated ratio R for large $-t$ is consistent with the s-channel quark model prediction of .25, and not with the u-channel prediction of 4. Clearly in σ_T the u-channel diagrams do not contribute in the forward direction. We might find similar evidence for the presense of PQCD backgrounds in this experiment by looking for a deviation of R_L from 1 .

An important prediction about this PQCD longitudinal response is that π^+ and π^0 electroproduction should have comparable magnitudes. This is completely different from the naive expectation that $\sigma_L \simeq 0$ for π^0 production since the t-pole diagram does not contribute. For this reason we have requested time to make measurements of forward π^0 electroproduction by detecting backward protons. Significant longitudinal response in forward π^0 electroproduction may be indicative of PQCD backgrounds in forward $\pi^\pm$ electroproduction.

A final important issue raised by Carlson and Milana [20] is the sensitivity of the extrapolated F_π to the $g_{\pi NN}$ form factor. Assuming a monopole representation

$$g_{\pi NN}(t) = g_{\pi NN}(0)/(1 - t/\Lambda^2_{\pi N})$$

we may expect significant variations in g for values of $-t_{min}$ which we will reach in this experiment. For example, for Q^2=2 $(GeV/c)^2$, W=2 GeV, we find that $-t_{min}$=.195 $(GeV/c)^2$. If Λ=1 GeV, then $g_{\pi NN}(.195)$ will be 16% lower than $g_{\pi NN}(0)$. (This would produce a similar size error in F_π.) Unfortunately, there is some controversy as to whether the large values of Λ derived from NN scattering are relevant to the isolated nucleon case, and some workers have argued for a much smaller value. [23] If this value were as small as Λ=.5 GeV, then $g_{\pi NN}(.195)$ would be 28% lower than in the Λ=1 GeV case.

This matter needs to be resolved, so we plan the following test. At $Q^2 = .5$ where we can access $-t_{min} \simeq m_\pi^2$, we will take high statistics data on $d\sigma_L/dt$ over a $-t$ range of several m_π^2. In this region there is no question about the dominant reaction mechanism and negligible model uncertainty. The only free parameters are F_π and $g_{\pi NN}(0)$, which together determine the overall scale, and Λ, which determines the decrease of $d\sigma_L/dt$ with $-t$ (ie, the shape). For $\Lambda \simeq$1.0 (0.5), $g_{\pi NN}$ will decrease about 2% (7%) for every $\Delta t = m_\pi^2$. Thus it should be easy to distinguish between these two extreme values of Λ in the planned range of $-t$. It is also likely that existing pion electroproduction data at small $-t$ may already tightly

constrain Λ, and we are looking into this. [24]

2 The Experiment

This examination of previous experiments, as well as the physics background considerations discussed in the Theory section, suggest several obvious ways in which a quality measurement of F_π could be done at CEBAF:

- Take high statistics data. This was not possible with the earlier low duty factor machines, and will make systematic errors easier to identify and control.
- At low Q^2 values, make careful measurements of $d\sigma_L/dt$ in $p(e,e'\pi^+)n$ for $-t \simeq +m_\pi^2$ in order to constrain the $g_{\pi NN}$ form factor. This would actually be the first important result of the experiment.
- Perform a separation of σ_L and σ_T for $p(e,e'\pi^+)n$ and $d(e,e'\pi^\pm)NN_s$. This decouples the F_π determination from the much more complicated transverse cross section. Do this in a manner which minimizes error amplification and extrapolation in Q^2 and W (eg, take the low and high ϵ points with the same apparatus during the same experiment).
- Measure the ratio $\sigma_L(\gamma_v + p \rightarrow \pi^+ + n)/\ \sigma_L(\gamma_v + n \rightarrow \pi^- + p)$ using a deuterium target to test for isoscalar backgrounds near the pion pole. This may also be useful for identifying PQCD backgrounds.
- Measure forward π^0 production (ie, backward proton production) in $\gamma_v + p \rightarrow p + \pi^0$ to look for PQCD background contributions to σ_L.
- Finally, where isoscalar or PQCD physics backgrounds are shown to be small, see whether σ_L is well described by the Born term model. If so, proceed to extract F_π.

In this experiment we will make coincidence measurements between charged pions or protons in the HMS and electrons in the SOS. Since the HMS will detect pions along the direction of $\vec{q}$, the dominant contribution will be due to the pion pole diagram. Only events with θ_{pq} near zero degrees are useful, so a high luminosity spectrometer system like the HMS-SOS is well suited to the measurement. Because σ_L must be separated, two beam energies are needed for each Q^2.

Table 1 contains the expected performance of each spectrometer in this experiment. If a large solid angle tune is used for the SOS (ie, point to point in Y), the target length acceptance is limited to at most 4 cm. This is adequate provided we use the 4 cm long

Table 1: Expected performance of the HMS (pt-to-pt, no Q1) and SOS (pt-to-pt).

	$\Delta p/p$	$\delta\theta$ (mrad)	$\delta\phi$ (mrad)	Δp (GeV/c)	$\Delta\Theta$ (mrad)	$\Delta\Phi$ (mrad)	$\Delta\Omega$ (msr)
HMS	10^{-3}	2	2	$\pm5\%$	±35	±21	3
SOS	10^{-3}	2	2	$\pm10\%$	±40	±50	8

cryotarget cells, do not move the SOS backward of about 60 degrees, and use only a $\pm10\%$ momentum bite. This will probably become the standard mode for running the SOS, so the acceptance should be well understood by the time we run this experiment. The relatively large in-plane angle provided by this tune will allow us to cover a large range of $-t$ with a single SOS setting.

A tune for the HMS which is point-to-point in Y will give adequate target acceptance and solid angle. The HMS first quad will be pushed back or removed to permit smaller hadron angles. These small hadron angles are conjugate to backward electron (SOS) angles, and so allowed increased coverage in ϵ, the virtual photon polarization. We have assumed in Table 1 and our count rate estimates that reaching HMS angles as small as 10 degrees will require removing the first quadrupole, Q1. This reduces the useful momentum bite to $\pm5\%$. Significant investment in understanding this tune will be invaluable not only for this and other L-T separation experiments; constraints on SOS out of plane operation will be reduced due to the lack of interference with the HMS Q1. The no-Q1 tune may even become standard if the CEBAF maximum beam energy is increased to 6 GeV and beyond.

A liquid hydrogen target will be used to make cross-section measurements of $\gamma_v + p \rightarrow \pi^+ + n$. We will use a liquid deuterium target to determine the separated ratio

$$R_L = \sigma_L(\gamma_v + n \rightarrow \pi^- + p)/\sigma_L(\gamma_v + p \rightarrow \pi^+ + n).$$

The Hall C cryogenic target will be used. The design is similar to that of a SLAC target by John Mark. Although the target heat exchangers are designed to provide 250 Watts of cooling power, we feel that a maximum beam load of 200 Watts is more realistic. This limits the maximum beam current to about 175 μA. It will be possible to rapidly change between liquid hydrogen, liquid deuterium, or empty vessels. The use of short, 4 cm long target cells will help minimize systematic errors caused by target acceptances changes with angle. The target windows will be viewed by both spectrometers at all angle settings, so target empty measurements must also be made.

Standard Hall C beamline hardware will be used. This includes the raster/deraster system, beam position monitors, and beam current monitors.

2.1 Kinematic Settings

Sample kinematic settings for $\pi^{\pm}$ detection are found in Table 2, assuming two phases of measurements. The invariant mass W is constrained to be 2 GeV/c^2. While these settings yield optimal ϵ coverage given the angular and momentum range of the SOS and HMS, other solutions are possible. For example, with some sacrifice in ϵ coverage, all of Phase 1 could be performed with only two beam energies. Similarly, there is some flexibility in the choice of Q^2 values. If CEBAF is to run in multi-user mode, then in general the beam energies and Q^2 values for experiments will be decided by scheduling constraints as well as by physics considerations. For our experiment, it is important that we be able to cover the proposed Q^2 range, and that we be permitted two energies at each Q^2 which provide adequate ϵ coverage. Given the opportunity, however, we would run the kinematics in the table.

We also wish to look for protons corresponding to forward π^0 production to search for PQCD related longitudinal backgrounds. These backgrounds might also be thought of as arising from minimally inelastic jets. There are two solutions to the proton momentum in $p(e,e'p)\pi^0$ at $\theta_{pq} = 0$ degrees. The higher momentum solution favors the amplitude for u-channel proton knockout, where the virtual photon is absorbed by an off-shell nucleon. While a complete understanding of pion electroproduction certainly requires an exploration of this kinematic regime, this is beyond the scope of this proposal. The lower proton momentum solution correspond to t-channel absorption of the virtual photon by a virtual pion. These momenta are generated at the $N \rightarrow N\pi$ vertex and produce easily detectable protons.

2.2 Rates

Our rate estimates are based on the following constraints:

- The target thickness 4 cm.
- The beam current on the 4 cm cryotarget cannot exceed 175 μA (ie, 200 Watt beam load).
- Assuming a coincidence timing window of 20 nsec, the online ratio of real coincidences to random coincidences should ideally be ≥ 1.
- The total trigger rate (reals + randoms + prescaled singles) assuming a 20 ns coincidence window should not exceed 1 kHz. Above this rate the data acquisition deadtime will increase dramatically. (We are actually far below this trigger rate in this proposal.)

Table 2: Kinematic settings for $N(e,e'\pi^{\pm})N$ and $p(e,e'p)\pi^0$ at Q^2=.5-5. and W = 2.

Q^2 $(GeV/c)^2$	P_e (GeV/c)	ϵ	$\theta_{e'}^{SOS}$ (deg)	θ_h^{HMS} (deg)	$P_{e'}^{SOS}$ (GeV/c)	P_{π}^{HMS} (GeV/c)	P_p^{HMS} (GeV/c)	$-t_{min}$ $(GeV/c)^2$
Phase I								
.50	2.7	.48	28.4	10.3	.77	1.91	.143	.020
	3.6	.74	16.6	13.4	1.67			
.75	2.7	.38	38.5	10.2	.64	2.04	.202	.040
	3.7	.70	20.3	14.7	1.64			
1.0	2.8	.33	45.2	10.2	.61	2.16	.257	.065
	3.9	.69	22.4	15.6	1.71			
1.5	3.1	.30	51.6	10.5	.64	2.39	.360	.125
	4.1	.63	27.3	15.9	1.64			
Phase II								
2.0	3.4	.27	55.8	10.4	.67	2.62	.453	.195
	4.4	.59	30.2	15.9	1.67			
3.0	4.0	.24	60.5	10.0	.74	3.07	.625	.354
	4.9	.52	35.6	15.0	1.64			
4.0	4.7	.26	58.0	10.3	.91	3.51	.781	.530
	5.5	.48	38.1	14.2	1.71			
5.0	5.4	.28	55.4	10.4	1.07	3.94	.929	.717
	6.0	.43	41.3	13.1	1.67			

Table 3: Real coincidence rate at $-t_{min}$ for the $N(e,e'\pi^{\pm})N$ kinematic settings. Only the pion pole contribution and σ_L are used, along with the F_π prediction of Jacob and Kisslinger. The number of hours has been rounded up to the nearest integer.

Q^2	$d\sigma_L/dt$ $(\mu b/GeV^2)$	Beam Current (μA)	Statistics Goal	Real Coinc. per Hour	Hours
Phase I					
.50	32.8	100	$1{\cdot}10^4$	$1.79{\cdot}10^4$	1.
			$1{\cdot}10^4$	$1.90{\cdot}10^5$	1.
.75	24.0		$1{\cdot}10^4$	$4.88{\cdot}10^3$	3.
			$1{\cdot}10^4$	$8.98{\cdot}10^4$	1.
1.0	14.9		$1{\cdot}10^4$	$1.93{\cdot}10^3$	6.
			$1{\cdot}10^4$	$4.88{\cdot}10^4$	1.
1.5	5.21		$1{\cdot}10^4$	$5.41{\cdot}10^2$	19.
			$1{\cdot}10^4$	$1.07{\cdot}10^4$	1.
Phase II					
2.0	2.15	175	$1.6{\cdot}10^3$	$2.02{\cdot}10^2$	5.
			$1.6{\cdot}10^3$	$3.72{\cdot}10^3$	1.
3.0	.528		$1.6{\cdot}10^3$	$4.80{\cdot}10^1$	19.
			$1.6{\cdot}10^3$	$6.36{\cdot}10^2$	2.
4.0	.166		$1.6{\cdot}10^3$	$2.40{\cdot}10^1$	38.
			$1.6{\cdot}10^3$	$1.87{\cdot}10^2$	5.
5.0	.0609		$1.6{\cdot}10^3$	$1.34{\cdot}10^1$	69.
			$1.6{\cdot}10^3$	$5.65{\cdot}10^1$	17.

The coincidence rate (Hz) assuming 100 μA on a 4 cm LH2 target (Luminosity = $1 \cdot 10^{38} cm^{-2} sec^{-1}$) is then:

$$R = (1.06 \cdot 10^8)\Gamma(\epsilon \frac{d\sigma_L}{dt})\Delta\Omega_e \Delta P_{e'} \Delta t$$

where $1.06 \cdot 10^8 = (1 \cdot 10^{38} cm^{-2} sec^{-1})(1 \cdot 10^{-30} cm^2/\mu barn)$. Spectrometer acceptances were already given in Table 1; count rate estimates are summarized in Table 3.

Singles rates in the HMS and SOS are given in Table 4 for $p(e,e'\pi^+)$ data taking. [22] The total singles rates are well below the expected capability of the detector packages, which are expected to have only a few percent electronic deadtime at 1 MHz. For the purpose of calculating random coincidence rates, the HMS trigger rate is taken as equal to the raw trigger rate. (We do not plan to distinguish pions and protons in the HMS online.) The SOS

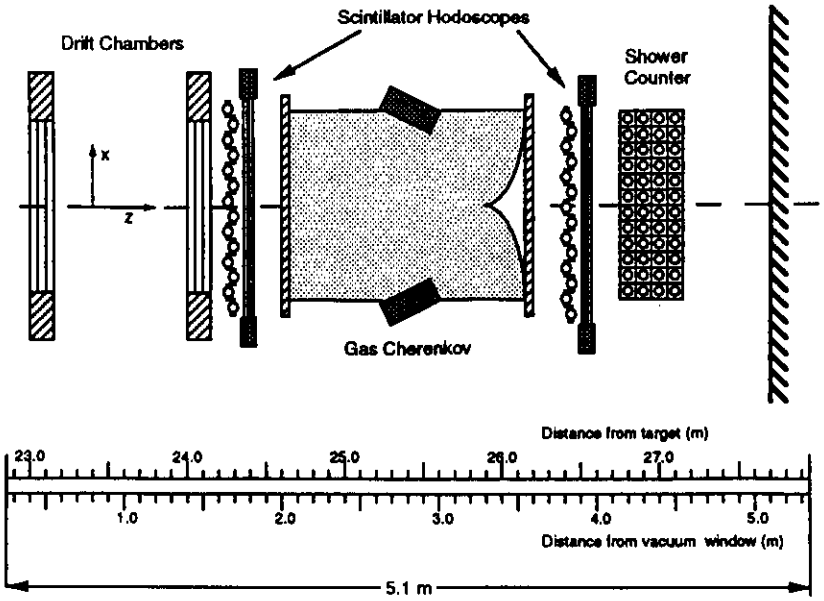

Figure 6: The HMS detector configuration. The SOS configuration will be similar for this experiment.

trigger rate is that for electrons only. The random coincidence rate is then given by (HMS trigger rate)(SOS trigger rate)Δt, where the coincidence resolving time $\Delta t = 20$ nsec. The table shows that *online* reals/randoms ratios are of order 1 for the Phase I measurements and in the range .1 - .5 for the Phase II measurements. This ratio will improve dramatically offline using a 2 nsec coincidence resolving time, and by placing cuts on the reconstructed mass of the undetected hadron.

We also examined the rates and reals/randoms ratios for $d(e,e'\pi^{\pm})$. The rates for the SOS and HMS were typically a factor of 1-2 larger for $d(e,e'\pi^{+})$ compared to $p(e,e'\pi^{+})$. Detection of negative pions in the HMS for $d(e,e'\pi^{-})$ is a different matter. Due to the electron background, the total HMS singles rates are larger than the Table 4 rates by an order of magnitude, up to about .5 MHz. This rate presents no problem in the HMS, but hardware rejection of the electrons is then necessary to minimize random coincidences. After electron rejection, the HMS trigger rate will be less than or equal to that for $p(e,e'\pi^{+})$ data taking. (There are no protons in this case.) In summary, the online reals/randoms ratio for deuterium data taking deteriorates from the Table 4 values by a factor ≤ 4 for $d(e,e'\pi^{+})$ and ≤ 2 for $d(e,e'\pi^{-})$.

2.3 Particle Identification

The HMS detector package will be configured for $\pi^{\pm}$ or proton detection in this experiment, and the HMS will sit at very forward angles. The two polarities for the HMS present

Table 4: Singles rates in the HMS and SOS, random coincidence rates (Δt = 20 nsec), and online reals/randoms ratio for $p(e, e'\pi^+)$. HMS triggers equals HMS singles since pions and protons are not distinguished online. The reals/randoms ratio will be greatly improved with offline cuts.

Q^2	HMS Rate $\pi^+ + p$ (Hz)	SOS Rate $e + \pi^-$ (Hz)	SOS Triggers $e's$ only (Hz)	Random Coinc. (Hz)	Reals/Randoms (Online)
Phase I					
.50	$4.9{\cdot}10^4$	$3.3{\cdot}10^5$	$7.4{\cdot}10^3$	7.3	.68
	$6.3{\cdot}10^4$	$2.3{\cdot}10^5$	$4.8{\cdot}10^4$	60.	.88
.75	$3.4{\cdot}10^4$	$2.3{\cdot}10^5$	$2.3{\cdot}10^3$	1.6	.85
	$4.0{\cdot}10^4$	$1.2{\cdot}10^5$	$2.1{\cdot}10^4$	17.	1.5
1.0	$2.8{\cdot}10^4$	$1.9{\cdot}10^5$	$1.1{\cdot}10^3$	.62	.85
	$2.8{\cdot}10^4$	$7.4{\cdot}10^4$	$1.3{\cdot}10^4$	7.3	1.9
1.5	$2.2{\cdot}10^4$	$1.2{\cdot}10^5$	$5.1{\cdot}10^2$	.22	.68
	$1.7{\cdot}10^4$	$3.7{\cdot}10^4$	$4.5{\cdot}10^3$	1.5	2.0
Phase II					
2.0	$3.2{\cdot}10^4$	$1.5{\cdot}10^5$	$5.1{\cdot}10^2$	.33	.17
	$1.9{\cdot}10^4$	$3.4{\cdot}10^4$	$4.0{\cdot}10^3$	1.5	.69
3.0	$2.5{\cdot}10^4$	$8.1{\cdot}10^4$	$2.1{\cdot}10^2$	.11	.12
	$1.1{\cdot}10^4$	$1.4{\cdot}10^4$	$1.2{\cdot}10^3$	.26	.68
4.0	$1.7{\cdot}10^4$	$3.6{\cdot}10^4$	$1.5{\cdot}10^2$	.051	.13
	$7.4{\cdot}10^3$	$6.7{\cdot}10^3$	$6.2{\cdot}10^2$	.092	.56
5.0	$1.2{\cdot}10^4$	$1.7{\cdot}10^4$	$1.0{\cdot}10^2$	.024	.16
	$5.6{\cdot}10^3$	$4.7{\cdot}10^3$	$2.9{\cdot}10^2$	.032	.49

very different cases for particle identification. When the HMS is tuned for a π^+, for example, the ratio π/p is of order 1. These particles will be distinguished offline using time of flight. However, when the HMS is tuned for π^-, the ratio e/π varies from 1 to 10. Hence, we must be able to reject electrons in hardware efficiently.

The detector stack will consist of two wire chambers followed by an X-Y scintillator hodoscope, a gas Cerenkov detector, another X-Y hodoscope, and finally a Pb-glass shower counter. (Figure 6) This configuration will be the same throughout the experiment. With the gas Cerenkov operated at sub-atmospheric pressure, only electrons will produce Cerenkov light. The gas Cerenkov will be used in the hardware trigger to reduce random coincidences. Offline the Pb glass shower counter will be used to further reduce electron contamination. Thus the gas Cerenkov and the Pb glass shower counter in combination will allow us to reject electrons with inefficiencies of $1 \cdot 10^{-5}$, orders of magnitude better than is needed. The primary (non-prescaled) HMS trigger for $\pi^{\pm}$ or p detection will be $(S1XOR \bullet S1YOR) \bullet (S2XOR \bullet S2YOR) \bullet (NoCerenkov)$.

Offline time of flight separation will be done as follows. First, the beam burst will be determined by the electron arm (SOS). Prototype 1 cm thick hodoscope elements for the HMS and SOS have meantime resolutions of $\sigma \simeq 70$ psec, so as long as SOS flight path corrections are made we can easily distinguish beam bursts which are 2 nsec apart. The hadron detected in the HMS will then be timed with respect to the accelerator RF. Given the 26 meter flight path through the HMS to the detector package, pions and protons will be separated for all kinematic settings.

The SOS detector package will be configured for electron detection. Because the SOS angle will vary from forward to backward angles, the ratio π^-/e varies varies from one to several hundred. It is especialy important that we be able to reject pions at the backward SOS angles, and by doing this in the hardware trigger we can reduce the online randoms rate. We can again use a sub-atmospheric pressure Cerenkov detector to discriminate between electrons and π^-'s. In this case the primary (non-prescaled) SOS trigger will be $(S1XOR \bullet S1YOR) \bullet (S2XOR \bullet S2YOR) \bullet Cerenkov$.

While the event of interest will be HMS•SOS, prescaled HMS and SOS singles events will also be taken in order to monitor the detector efficiencies and luminosity.

2.4 Non-physics backgrounds

Once a combination of on-line hardware and off-line software have determined that there was a coincidence between an electron in the SOS and a hadron in the HMS (a pion or proton depending on the reaction), there remain several backgrounds of the incoherent 'non-physics' variety: random coincidences and events from the target endcaps.

The online coincidence resolving window will be roughly 20 ns. Because the offline analysis will allow the beam burst to be determined, the relevant resolving time becomes 2 ns. This alone reduces the online random coincidences by 90%. Some of the remaining randoms may be removed with vertex cuts, but most randoms will be removed with missing mass cuts. The mass of the residual (ie, undetected) hadron may be reconstructed from the final electron and detected hadron 4-momenta:

$$M_{res}^2 = P_{res}^2 = (P_e - P_{e'} + P_{tgt} - P_h)^2$$

A cut on this missing mass variable would remove backgrounds with larger inelasticity, such as two pion production.

We have chosen the target length to be relatively short. This means that both spectrometers will view the endwindows in all configurations, so background runs and subtractions will be necessary. Assuming that the aluminum windows are each 4 mils thick, the ratio of protons in the windows to protons in the liquid hydrogen is about 10%. Therefore roughly $\sqrt{(.10)} \simeq 1/3$ of the running time will be devoted to empty target runs.

2.5 Beam Request

The beam request assumes $1{\cdot}10^4$ counts per kinematic setting for the Phase I points (low Q^2, assuming 1% statistics), and $1.6{\cdot}10^3$ counts for the Phase II points (high Q^2, 2.5% statistics). We take $p(e,e'\pi^+)$ and $p(e,e'p)\pi^0$ running times on LH2 to be equal. (Although the PQCD backgrounds may turn out to be relatively small, the Jacobian for backward proton production is unfavorable, so we need running times of the same order.) We also take the $p(e,e'\pi^+)$ and $d(e,e'\pi^\pm)NN_s$ running times to be equal so that accurate values of the separated ratios $\sigma(\pi^-)/\sigma(\pi^+)$ can be obtained. Additional time is requested for target background runs, and overhead. Overhead was calculated assuming 12 hours per kinematic setting (ie, time to change the beam energy, the spectrometer angles, survey the spectrometer angles, and reverse the dipole polarity). A summary of the beam request is contained in Table 5. *We request 9 beam days for Phase I and 90 beam days for Phase II, for a total request of 99 beam days.*

2.6 Errors

Two measurements at fixed (Q^2, W) and different values of ϵ, the virtual photon polarization, are needed in order to determine σ_L. Thus if $\sigma_1 = \sigma_T + \epsilon_1\sigma_L$ and $\sigma_2 = \sigma_T + \epsilon_2\sigma_L$ then

$$\sigma_L = \frac{1}{\epsilon_1 - \epsilon_2}(\sigma_1 - \sigma_2).$$

Table 5: Beam Request for hydrogen and deuterium running.

Q^2	LH2 Hours $p(e,e'\pi^+)$	LH2 Hours $p(e,e'p)\pi^0$	LD2 Hours $d(e,e'\pi^\pm)$	Background Hours	Overhead Hours	Total Hours
Phase I						
.50	1	1	1	1	0	4
	1	1	1	1	12	16
.75	3	3	3	3	12	24
	1	1	1	1	12	16
1.0	6	6	6	6	12	36
	1	1	1	1	12	16
1.5	19	19	19	19	12	88
	1	1	1	1	12	16
					Total I	216
Phase II						
2.0	5	5	5	5	12	32
	1	1	1	1	12	16
3.0	19	19	19	19	12	88
	2	2	2	2	12	20
4.0	38	38	38	38	12	164
	5	5	5	5	12	32
5.0	69	69	69	69	12	288
	17	17	17	17	12	80
					Total II	720
					Total I+II	936

Assuming uncorrelated errors in the measurement of σ_1 and σ_2, then

$$\frac{\Delta\sigma_L}{\sigma_L} = \frac{1}{(\epsilon_1 - \epsilon_2)}\frac{1}{\sigma_L}\sqrt{\Delta\sigma_1^2 + \Delta\sigma_2^2}.$$

A more insightful expression is obtained by defining $R \equiv \sigma_T/\sigma_L$ and $\Delta\sigma/\sigma \equiv \Delta\sigma_1/\sigma_1 = \Delta\sigma_2/\sigma_2$, then

$$\frac{\Delta\sigma_L}{\sigma_L} = \frac{1}{\epsilon_1 - \epsilon_2}\frac{\Delta\sigma}{\sigma}\sqrt{(R+\epsilon_1)^2 + (R+\epsilon_2)^2}$$

This equation makes explicit the error amplification due to a limited ϵ range as well as a large R. For the proposed experiment, $R \leq 1$, so a limited ϵ lever arm is the primary source of error amplification. Systematic errors in the kinematic factors (ie, Γ, Q^2, W^2, and ϵ) are small provided we determine the absolute P_e to $1 \cdot 10^{-3}$ and the centroids of laboratory scattering angles to 1 mrad.

Based on the experience of the SLAC group [21], it will require a great deal of effort at CEBAF to achieve 2% absolute cross section errors with extended targets and magnetic spectrometers with multiple solid angle-defining apertures. The SLAC estimate of 2% systematic errors was obtained by adding the errors in target thickness, acceptance, beam charge, and radiative corrections in quadrature:

$$\sqrt{.01^2(target) + .01^2(acceptance) + .01^2(charge) + .01^2(rad.corr.)} = 2\%.$$

We believe a reasonable goal for the error $\Delta\sigma/\sigma$ for the early years at CEBAF is

$$\sqrt{.02^2(target) + .02^2(acceptance) + .005^2(charge) + .01^2(rad.corr.)} \sim 3\%.$$

Table 6 gives our anticipated errors for the entire Q^2 range, including both systematic and statistical errors. Statistical errrors are negligible for the low Q^2 Phase I measurements, but rapidly increase with Q^2 for the Phase II measurements.

Assuming the absolute cross section error appropriate for CEBAF, and a value of .1 (.5) for σ_T/σ_L for the low (high) Q^2 settings, then $\Delta\sigma_L/\sigma_L = 8.0\%$ (32%). Since $\sigma_L \propto F_\pi^2$ we have

$$\frac{\Delta F_\pi}{F_\pi} = \frac{1}{2}\frac{\Delta\sigma_L}{\sigma_L} = 4.0\% - 16\%.$$

We would like to point out that if errors in the measurement of σ_1 and σ_2 are correlated (eg, the beam current monitor calibration is consistently .5% low) then the error in F_π will be smaller than that given above. However, our error estimates neglect any model uncertainties and physics backgrounds. We will determine these in the experiment and include these in the final published errors on F_π. For example, we propose to measure the $g_{\pi NN}$ form factor and will spend a significant fraction of the running time looking for physics backgrounds. Given these caveats, our expected uncertainties are shown in Figure 7.

Table 6: Expected errors for F_π in the proposed experiment. Model errors are not included.

Q^2	Systematic (%)	Statistical (%)	$\Delta\sigma/\sigma$ (%)	σ_T/σ_L	$\Delta F_\pi/F_\pi$ (%)
Phase I					
.50	3	1	3.2	.1	6.3
.75	3	1	3.2	.1	4.7
1.0	3	1	3.2	.1	4.0
1.5	3	1	3.2	.1	6.7
Phase II					
2.0	3	2.5	3.9	.5	8.1
3.0	3	2.5	3.9	.5	8.8
4.0	3	2.5	3.9	.5	11.
5.0	3	2.5	3.9	.5	16.

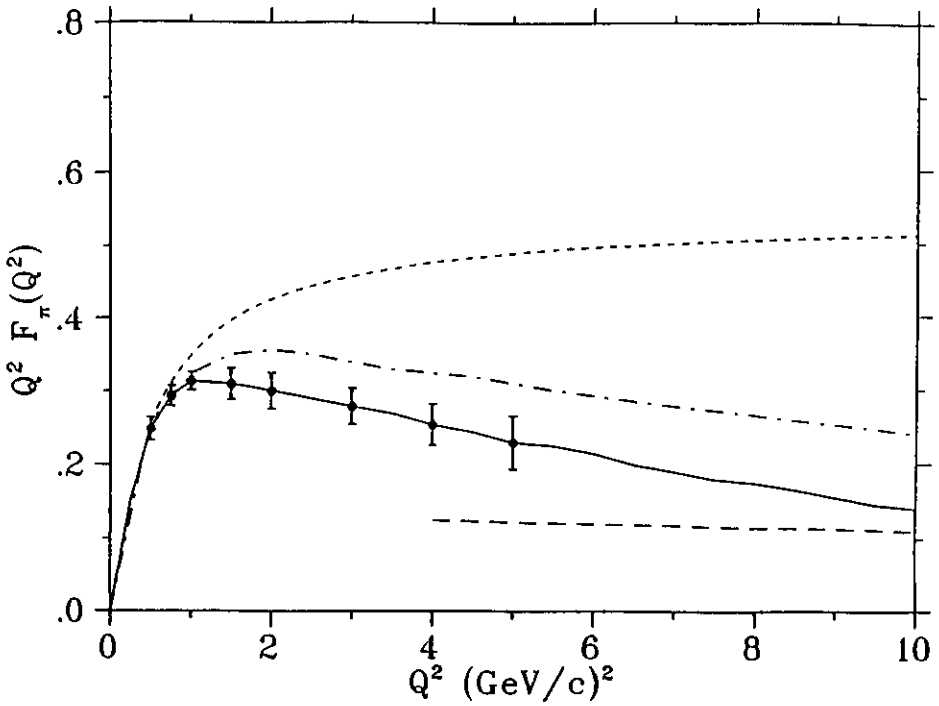

Figure 7: Our *anticipated* errors for F_π assuming the Bethe-Salpeter equation model of Jacob and Kisslinger (solid line). The other theory curves are the same as in Figure 3.

2.7 The Collaboration

We believe our collaboration has the strength and commitment to successfully carry out these measurements. Hampton University has a proposal to study the electroproduction of K^+ at large Q^2, and Napolitano (now at RPI) long ago submitted a Letter of Intent to measure F_π. Yerevan is submitting to this PAC a proposal to measure $A(e, e'\pi^+)$ in the deep inelastic regime. Each institution is building hardware which will be employed in the experiment: Hampton University is building wire chambers for the HMS, Old Dominion University is building scintillator hodoscopes for the SOS, RPI is building an aerogel Cerenkov detector for the SOS, and Yerevan is building the shower counters for the HMS and SOS. CEBAF staff scientists assist in these projects and are responsible for electronics, data acquisition, and beamline hardware.

3 Summary

At CEBAF we have the potential to dramatically improve the F_π database. Much can be learned from the proposed experiment about the usefulness of QCD sum rules and relativistic potential models for understanding the structure of the pion in the (presumably) difficult and non-perturbative Q^2 regime of 1-5 $(GeV/c)^2$.

All the hardware required for the proposed experiment is expected to be available in the endstation at startup. Furthermore, the requirements on momentum resolution and

angular resolution are very modest, as is the requirement on absolute determination of the scattering angles. The detector packages we require are standard equipment for the HMS and SOS. The particle identification capabilities of the detector packages as we have described them are several orders of magnitude better than what is necessary, and the count rates are reasonable. In conclusion, Phase I of these important measurements could be made in endstation C shortly after startup. The Phase II measurements definitely require beam over 4 GeV.

References

[1] S.R.Amendolia et al., PL **146B**, 116 (1984); NPB**277**, 168 (1986). G.T. Adylov et al., PL **51B**, 402 (1974); NPB**128**, 461 (1977). E.B. Dally et al., PRL **39**, 1176 (1977); PRD **24**, 1718 (1981). E.B. Dally et al. PRL **48**, 375 (1982).

[2] P. Brauel et al., Z. Physik C, **3**, 101 (1979)

[3] M. Helm, Dissertation zur Erlangung des Doktorgrades, Universitaet Hamburg, 1978. (Interner Bericht DESY F22-78/03 Mai 1978)

[4] M. Schaedlich, Dissertation zur Erlangung des Doktorgrades, Universitaet Hamburg, 1976. (Interner Bericht DESY F22-76/02 November 1976)

[5] Brown et al., Phys. Rev. D **8**, 92 (1973)

[6] F.A. Berends, Phys. Rev. D **1**, 2590 (1970)

[7] C.J. Bebek et al., Phys. Rev. D **9**, 1229 (1974)

[8] C.J. Bebek et al., Phys. Rev. D **13**, 25 (1976)

[9] C.J. Bebek et al., Phys. Rev. Lett. **37**, 1326 (1976); and Phys. Rev. D **17**, 1693 (1978)

[10] O. Nachtman, Nucl. Phys. **B115** 61 (1976).

[11] N. Isgur and C.H. Llewellyn Smith, Phys. Rev. Lett. **52**, 1080 (1984), Phys. Lett. **B217**, 535 (1989), and Nucl. Phys. **B317** 526 (1989).

[12] A.P. Bakulev and A.V. Radyushkin, CEBAF preprint.

[13] S.V. Mikhailov and A.V. Radyushkin, CEBAF preprint.

[14] O.C. Jacob and L.S. Kisslinger, Phys. Lett. B **243**, 323 (1990).

[15] G. R. Farrar and D. R. Jackson, Phys. Rev. Lett. **43**, 246 (1979).

[16] H. Ito et al., Phys. Rev C **45**, 1918 (1992).

[17] C.-R. Ji and F. Amiri, Phys. Rev. D **42** 3764 (1990).

[18] T. Draper, R.M. Woloshyn, W. Wilcox, and K.-F. Liu, Nucl. Phys. **B318**, 319 (1989).

[19] W. Wilcox, private communication.

[20] C.E. Carlson and J. Milana, Phys. Rev. Lett. **65**, 1717 (1990).

[21] P.E. Bosted et al., Phys. Rev. Lett. **68**, 3841 (1992).

[22] J. O'Connell and J. Lightbody, Comp. in Phys. May-June **57** (1988)

[23] A.W. Thomas and K. Holinde, Phys. Rev. Lett. **63**, 2025 (1989).

[24] D. Mack, to be published.